

Formation of a vortex lattice in a rotating BCS Fermi gas

Giulia Tonini¹ and Yvan Castin^{2,*}

¹*Dipartimento di fisica, Università di Firenze, Firenze, Italy*

²*Laboratoire Kastler Brossel, École Normale Supérieure,*

24 rue Lhomond, 75231 Paris Cedex 05, France

(Dated: December 2, 2024)

We investigate theoretically the formation of a vortex lattice in a superfluid two-spin component Fermi gas in a rotating harmonic trap, in a two-dimensional geometry and in a quite strongly interacting BCS-type regime. Our analytical solution of the superfluid hydrodynamic equations predicts that the vortex free gas is subject to a dynamic instability for fast enough rotation. With a numerical solution of the full time dependent BCS equations, we confirm the existence of this dynamic instability and we show that it leads to the entrance of quantum vortices in the gas.

PACS numbers: 03.75.Fi, 02.70.Ss

The field of trapped ultracold fermionic atomic gases is presently making rapid progress: thanks to the possibility of controlling at will the strength of the s-wave interaction between two different spin components by the technique of the Feshbach resonance [1, 2], it is possible to investigate the cross-over [3] between the weakly interacting BCS regime (case of a small and negative scattering length) and the Bose-Einstein condensation of dimers (case of small and positive scattering length), including the strongly interacting regime and even the unitary quantum gas (infinite scattering length). The interaction energy of the gas was measured on both sides of the Feshbach resonance [2]; on the side of the resonance with a positive scattering length, Bose-Einstein condensation of dimers was observed [4]; on the side of the resonance with a negative scattering length, a condensation of pairs was revealed in the strongly interacting regime by a fast ramping of the magnetic field across the Feshbach resonance [5]. Also, the presence of a gap in the excitation spectrum was observed [6], for an excitation consisting in transferring atoms to an initially empty atomic internal state, as initially suggested by [7], revealing pairing.

Are there evidences of superfluidity in these fermionic gases? It was initially proposed [8] to reveal superfluidity by detecting an hydrodynamic behavior in the expansion of the gas after a switching-off of the trapping potential. Such an hydrodynamic behavior was indeed observed [1] but it was then realized that such a behavior can occur not only in the superfluid phase, but also in the normal phase in the so-called hydrodynamic regime, that is when the mean free path of atoms is smaller than the size of the cloud, a condition easy to fulfill close to a Feshbach resonance. The general trend is now to try to detect superfluidity via an hydrodynamic behavior that has no counterpart in the normal phase [9]. A natural candidate to reveal superfluidity is therefore the detection of quantum vortex lattices in the rotating trapped Fermi gases: the superfluid velocity field, defined as the gradi-

ent of the phase of the order parameter, is irrotational everywhere, except on singularities corresponding to the vortex lines, so that a superfluid may respond to rotation by the formation of a vortex lattice [10]; on the contrary, a rotating hydrodynamic normal gas is expected to acquire the velocity field of solid-body rotation and should not exhibit a regular vortex lattice in steady state.

Steady state properties of vortices in a rotating Fermi gas described by BCS theory have already been the subject of several studies, for a single vortex configuration [11] and more recently for a vortex lattice configuration [10]. In this paper, we study the issue of the time dependent formation of the lattice in a rotating Fermi gas, by solving the time dependent BCS equations. A central point of the paper is to identify possible nucleation mechanisms of the vortices that could show up in a real experiment.

This problem was addressed a few years ago for rotating Bose gases. The expected nucleation mechanism was the Landau mechanism, corresponding to the apparition of negative energy surface modes for the gas in the rotating frame, for a rotation frequency above a critical value; these negative energy modes can then be populated thermally, leading to the entrance of one or several vortices from the outside part of the trapped cloud [12, 13]. The first experimental observation of a vortex lattice in a rotating Bose-Einstein condensate revealed however a nucleation frequency different from the one of the thermal Landau mechanism [14] and was understood later on to be due to a dynamic instability of hydrodynamic nature triggered by the rotating harmonic trap [15, 16, 17]. The discovered mechanism of dynamic instability was checked, by a numerical solution of the purely conservative time dependent Gross-Pitaevskii equation, to lead to turbulence [18] and to the formation of a vortex lattice [19].

We now transpose this problem to the case of a two spin component Fermi gas in two dimensions, initially at zero temperature and stirred by a rotating harmonic trapping potential of slowly increasing rotation speed, as described in section I. Does the hydrodynamic instability phenomenon occur also in the fermionic case, and

*Electronic address: yvan.castin@lkb.ens.fr

does it lead to the entrance of vortices in the gas and to the subsequent formation of a vortex lattice? We first address this problem analytically, in section II, by solving exactly the time dependent two-dimensional hydrodynamic equations and by performing a linear stability analysis: very similarly to the bosonic case, we find that a dynamic instability can occur above some minimal rotation speed. Then we test this prediction by a numerical solution of the time dependent BCS equations on a two-dimensional lattice model, in section III: this confirms that the dynamic instability can take place and leads to the entrance of vortices in the gas, which are then seen to arrange in a vortex lattice. Furthermore, the numerical simulations show that the vortex lattice can also form for a lower rotation frequency than the one predicted analytically, by a different and slower mechanism not involving turbulence; as we shall discuss, our present simulations cannot exclude the fact that this mechanism may be enhanced or even activated by the finite size of the rotating quantization box used in the simulations.

I. OUR MODEL

We consider a gas of fermionic particles of mass m , with equally populated two spin states \uparrow and \downarrow , trapped in a harmonic potential and initially at zero temperature. The particles with opposite spin have a s -wave interaction with a negligible range interaction potential, characterized by the scattering length a_{3D} , whereas the particles in the same spin state do not interact.

The trapping potential is very strong along z axis so that the quantum of oscillation along z , that is $\hbar\omega_z$, where ω_z is the oscillation frequency along z , is much larger than the mean oscillation energy in the $x-y$ plane plus the interaction energy, so that the gas is dynamically frozen along z in the ground state of the corresponding harmonic oscillator. Furthermore, we assume that the spatial extension $(\hbar/m\omega_z)^{1/2}$ of the ground state of this harmonic oscillator is smaller than a_{3D} so that the interactions between the particles acquire a true two-dimensional character. The resulting 2D interaction can be characterized by the 2D scattering length a_{2D} which was calculated as a function of the 3D scattering length in [20, 21]. We recall that a_{2D} is always strictly positive in the true 2D regime and the two-body problem in free space exhibits a bound state, that is a dimer, of spatial radius a_{2D} . The weakly attractive Fermi gas limit corresponds in 2D to $a_{2D} \rightarrow +\infty$ and the condensation of preformed dimers to $a_{2D} \rightarrow 0$ [22].

In the $x-y$ plane, the zero temperature 2D gas is initially harmonically trapped in the non-rotating, anisotropic potential

$$U(\mathbf{r}) = \frac{1}{2}m\omega^2 [(1-\epsilon)x^2 + (1+\epsilon)y^2] \quad (1)$$

where $\mathbf{r} = (x, y)$ and $\epsilon > 0$ measures the anisotropy of the trapping potential. Then one gradually sets the trapping

potential into rotation around z axis with an instantaneous rotation frequency $\Omega(t)$, until it reaches a maximal value Ω to which it then remains equal. The question is to study the resulting evolution of the gas and predict the possible formation and subsequent crystallization of quantum vortices.

We shall consider this question within the approximate frame of the BCS theory, in a rather strongly interacting regime but closer to the weakly interacting BCS limit than to the BEC limit, which is most relevant for the present 3D experimental investigations: the chemical potential μ of the 2D gas is supposed to be positive, excluding the regime of Bose-Einstein condensation of the dimers, and the parameter $k_F a_{2D}$, where the Fermi momentum is defined as $\hbar^2 k_F^2 / 2m = \mu$, is larger than unity but not extremely larger than unity: we shall take $k_F a_{2D} = 4$ in the numerical simulations. In this relatively strongly interacting regime, we of course do not expect the BCS theory to be 100% quantitative.

In the hydrodynamic approach to come, one simply needs the equation of state of the 2D gas, that is the expression of the chemical potential μ_0 of a spatially uniform zero temperature gas as a function of the density per spin component $\rho_\uparrow = \rho_\downarrow$ and of the 2D scattering length. This equation of state was calculated with the BCS approach in [22]:

$$\mu_0[\rho_\uparrow] = \frac{2\pi\hbar^2\rho_\uparrow}{m} - E_0/2 \quad (2)$$

where E_0 is the binding energy of the dimer in free space,

$$E_0 = \frac{4\hbar^2}{ma_{2D}^2 e^{2\gamma}} \quad (3)$$

and $\gamma = 0.57721\dots$ is Euler's constant. Similarly, the gap for the zero temperature homogeneous BCS gas is related to the density by [22]

$$\Delta_0[\rho_\uparrow] = \left(E_0 \frac{4\pi\hbar^2\rho_\uparrow}{m} \right)^{1/2}. \quad (4)$$

In the numerical solution of the time dependent BCS equations to come, one needs an explicit microscopic model. We have chosen a square lattice model with an on-site interaction between opposite spin particles corresponding to a coupling constant g_0 so that the second quantized grand canonical Hamiltonian reads at the initial time

$$\begin{aligned} H = & \sum_{\mathbf{k},\sigma} \left(\frac{\hbar^2 k^2}{2m} - \mu \right) c_{\mathbf{k},\sigma}^\dagger c_{\mathbf{k},\sigma} + \sum_{\mathbf{r},\sigma} l^2 U(\mathbf{r}) \psi_\sigma^\dagger(\mathbf{r}) \psi_\sigma(\mathbf{r}) \\ & + g_0 \sum_{\mathbf{r}} l^2 \psi_\uparrow^\dagger(\mathbf{r}) \psi_\downarrow^\dagger(\mathbf{r}) \psi_\downarrow(\mathbf{r}) \psi_\uparrow(\mathbf{r}) \end{aligned} \quad (5)$$

where l is the grid spacing. In the numerics a quantization volume is introduced, in the form of a square box of size L with periodic boundary conditions, L being an integer multiple of l . The sum over \mathbf{r} then runs over the

$(L/l)^2$ points of the lattice. A plane wave on the lattice has wavevector components k_x and k_y having a meaning modulo $2\pi/l$ so that the wavevector \mathbf{k} is restricted to the Brillouin zone $D = [-\pi/l, \pi/l]^2$. The operator $c_{\mathbf{k},\sigma}$ annihilates a particle of wavevector \mathbf{k} and spin state $\sigma = \uparrow$ or \downarrow , and obeys the usual fermionic anticommutation relations, such as

$$\{c_{\mathbf{k},\sigma}, c_{\mathbf{k}',\sigma'}^\dagger\} = \delta_{\mathbf{k},\mathbf{k}'}\delta_{\sigma,\sigma'}. \quad (6)$$

The discrete field operator $\psi_\sigma(\mathbf{r})$ is proportional to the annihilation operator of a particle at the lattice node \mathbf{r} in the spin state σ in such a way that it obeys the anticommutation relations

$$\{\psi_\sigma(\mathbf{r}), \psi_{\sigma'}^\dagger(\mathbf{r}')\} = l^{-2} \delta_{\mathbf{r},\mathbf{r}'} \delta_{\sigma,\sigma'}. \quad (7)$$

The coupling constant g_0 is adjusted so that the scattering length of two particles on the infinite lattice is exactly a_{2D} [23, 24]:

$$\frac{1}{g_0} = \frac{m}{2\pi\hbar^2} \left[\log\left(\frac{l}{\pi a_{2D}}\right) - \gamma + \frac{2G}{\pi} \right] \quad (8)$$

where $G = 0.916\dots$ is Catalan's constant.

At later times, the Hamiltonian is written in the frame rotating at frequency $\Omega(t)$, to eliminate the time dependence of the trapping potential; this adds an extra term to the Hamiltonian,

$$H_{\text{rot}} = -\Omega(t) \sum_{\mathbf{r},\sigma} l^2 \psi_\sigma^\dagger(\mathbf{r}) L_z \psi_\sigma \quad (9)$$

where the matrix L_z on the lattice represents the angular momentum operator along z , $xp_y - yp_x$. The square box defining the periodic boundary conditions is supposed to be fixed in the rotating frame, so that it rotates in the lab frame: this may be useful in practice to ensure that truncation effects due to the finite size of this box in the numerics do not arrest the rotation of the gas.

This lattice model is expected to reproduce a continuous model with harmonic trapping and zero range interaction potential in the limit of an infinite quantization volume ($L \gg$ spatial radius of the cloud) and in the limit of a vanishing grid size $l \rightarrow 0$ ($l \ll a_{2D}, k_F^{-1}$). In this limit g_0 is negative, $g_0 \rightarrow 0^-$, leading to an attractive interaction, so that pairing can take place in the lattice model. In this limit, we have checked that BCS theory for the lattice model gives the same equation of state as Eq.(2) [25].

II. SOLUTION TO THE SUPERFLUID HYDRODYNAMIC EQUATIONS

In the hydrodynamic theory of a pure superfluid with no vortex, one introduces two fields, the spatial density of the gas, here taken in a given spin state, $\rho_\uparrow(\mathbf{r}, t)$, and the phase of the so-called order parameter, $2S(\mathbf{r}, t)/\hbar$. In the

BCS theory for the lattice model, the order parameter is simply

$$\Delta(\mathbf{r}, t) \equiv -g_0 \langle \psi_\uparrow(\mathbf{r}, t) \psi_\downarrow(\mathbf{r}, t) \rangle \equiv |\Delta| e^{2iS/\hbar} \quad (10)$$

which has a finite limit when $l \rightarrow 0$. The superfluid velocity field in the lab frame is then defined as

$$\mathbf{v} = \frac{\mathbf{grad} S}{m}. \quad (11)$$

In the rotating frame, the hydrodynamic equations read

$$\partial_t \rho_\uparrow = -\text{div} [\rho_\uparrow (\mathbf{v} - \Omega(t) \times \mathbf{r})] \quad (12)$$

$$\begin{aligned} -\partial_t S = & \frac{1}{2} m v^2 + U(\mathbf{r}) + \mu_0 [\rho_\uparrow(\mathbf{r})] \\ & - \mu - m(\Omega(t) \times \mathbf{r}) \cdot \mathbf{v} \end{aligned} \quad (13)$$

where $\Omega(t) = \Omega(t)\hat{\mathbf{z}}$ and $\hat{\mathbf{z}}$ is the unit vector along the rotation axis z . The first equation is simply the continuity equation in the rotating frame, including that the velocity field in the rotating frame differs from the one in the lab frame by the solid body rotational term. When one takes the gradient of the second equation, one recovers Euler's equation for a superfluid. These superfluid equations are expected to be correct for a slowly varying density and phase, both in space (as compared to the size of pair) and in time (as compared to $\hbar/|\Delta|$). In the appendix A we present a simple derivation of these equations starting from the time dependent BCS theory and using the lowest order semi-classical approximation; this derivation explicitly uses the mentioned slow time variation. In the present paper, considering the rather strongly interacting regime $1 \lesssim k_F a_{2D}$, the pair size is on the order of k_F^{-1} much smaller than the cloud size, so that the slow spatial variation is satisfied as long as no vortex enters the cloud; the gap is a fraction of the Fermi energy, which is much larger than \hbar over the ramping time of the trap rotation, so that the expected condition of slow time variation is also satisfied. Surprisingly, our simple derivation requires an extra condition: both \hbar over the ramping time and the quantum of oscillation $\hbar\omega$ should be smaller than Δ^2/μ , that is (in 2D) than the free space dimer binding energy, a condition satisfied in our simulations.

We shall assume here that the rotation frequency is ramped up very slowly so that the density and the phase adiabatically follow a sequence of vortex free stationary states. The strategy then closely follows the one already developed in the bosonic case [15]: one solves analytically the corresponding stationary hydrodynamic equations, then one performs a linear stability analysis of the stationary solution. The apparition of a dynamic instability suggests that the system may evolve far away from the stationary branch; that this dynamic instability results in the entrance of vortices will be checked by the numerical simulations of section III.

In the stationary regime, for a fixed rotation frequency Ω , one sets $\partial_t \rho_\uparrow = 0$ in Eq.(12) and $-\partial_t S = 0$ in Eq.(13)

[26]. One replace μ_0 by the equation of state Eq.(2): apart from an additive constant, μ_0 is proportional to the density, as was the case for the weakly interacting condensate of bosons [15], so that the calculations for the superfluid fermions are formally the same, if one replaces the coupling constant g of the bosons by $2\pi\hbar^2/m$. Since the properties of the bosons do not depend on the value of g up to a scaling on the density [15], the results for the bosons can be directly transposed. Following [27], we take the ansatz for the phase:

$$S(\mathbf{r}) = m\omega\beta xy \quad (14)$$

which is applicable for a harmonic trapping potential U . When inserted in Eq.(13), this leads to an inverted parabola for the density profile, resulting in an elliptic boundary for the density of the cloud. Upon insertion of the density profile in the continuity equation, one recovers the cubic equation of [27]:

$$\beta^3 + \left(1 - 2\frac{\Omega^2}{\omega^2}\right)\beta - \epsilon\frac{\Omega}{\omega} = 0. \quad (15)$$

This equation has one real root for Ω below some ϵ dependent bifurcation value $\Omega_{\text{bif}}(\epsilon)$, and has three real roots for $\Omega > \Omega_{\text{bif}}(\epsilon)$. In figure 1, we have plotted β as a function of Ω/ω , for the value of the asymmetry parameter in the simulations of the next section, $\epsilon = 0.1$. In the considered stirring procedure, the system starts with $\beta = 0$ and follows adiabatically the upper branch of solution, corresponding to increasing values of β . When β takes appreciable values, the cloud significantly deforms itself in real space, becoming broader along x axis than along y axis, even for an arbitrarily weak trap anisotropy ϵ .

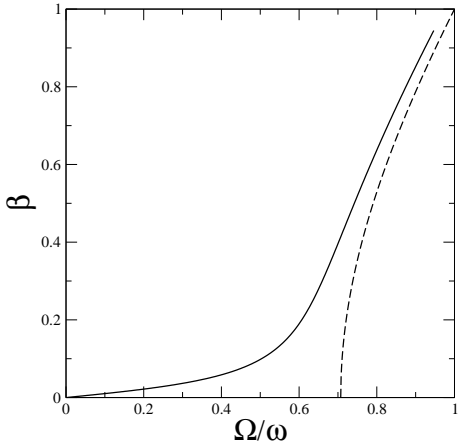


FIG. 1: The phase parameter β of the hydrodynamic approach for a stationary vortex free BCS state in the rotating frame, as a function of the rotation frequency. Solid line: the trap anisotropy is $\epsilon = 0.1$. Dashed line: $\epsilon = 0$.

From the studies of the bosonic case [15] it is known that the significantly deformed clouds can become dynamically unstable. We recall briefly the calculation procedure: one introduces initially arbitrarily small deviations $\delta\rho_\uparrow$ and δS of the density and the phase from their

stationary values; one then linearizes the hydrodynamic equations Eq.(12) and Eq.(13) to get

$$\frac{D\delta\rho_\uparrow}{Dt} = -\text{div}\left(\rho_\uparrow \frac{\mathbf{grad}\delta S}{m}\right) - \delta\rho_\uparrow \frac{\Delta_{\mathbf{r}}S}{m} \quad (16)$$

$$\frac{D\delta S}{Dt} = -\frac{2\pi\hbar^2}{m}\delta\rho_\uparrow \quad (17)$$

where $\Delta_{\mathbf{r}}$ stands for the 2D Laplacian and $D/Dt \equiv \partial_t + (\mathbf{v} - \Omega \times \mathbf{r}) \cdot \mathbf{grad}$. Note that the last term in Eq.(16) vanishes here since $S \propto xy$. One then calculates the eigenmodes of the linearized equations, setting $\partial_t \rightarrow -i\nu$ where ν is the eigenfrequency of the mode, and taking a polynomial ansatz of arbitrary total degree n for $\delta\rho_\uparrow$ and δS in the variables x and y . Since the stationary values ρ_\uparrow and S are quadratic functions of x and y , one can check that the subspace of polynomials of degree less than or equal to n is indeed stable. This turns the linearized partial differential equations into a finite size linear system whose eigenvalues can be calculated numerically. Complex eigenfrequencies, when obtained, lead to a non-zero Lyapunov exponent $\lambda \equiv \text{Im } \nu$, which reveals a dynamical instability when $\lambda > 0$.

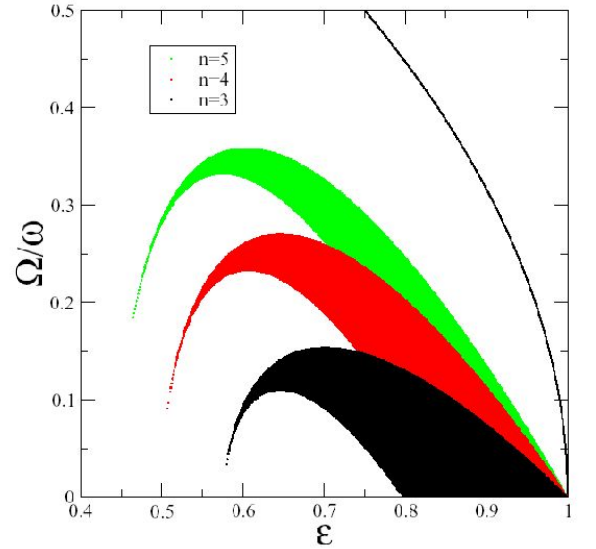


FIG. 2: For the upper branch of solution for the phase parameter: Dark areas: instability domain in the $\Omega - \epsilon$ plane for degrees n equal to 3, 4 and 5 (crescents from bottom to top). There is no dynamical instability for $n \leq 2$. Solid line: border $\Omega^2 = (1 - \epsilon)\omega$ of the branch existence domain.

In figure 2 we plot the stability diagram of the upper branch stationary solution in the plane (Ω, ϵ) , for various total degrees n of the polynomial ansatz. Each degree contributes to this diagram in the form of a crescent, touching the horizontal axis ($\epsilon = 0$) with a broad basis on the right side and a very narrow tongue on the left side [28]. For the low values of ϵ considered in the figure 1, the Lyapunov exponents in the tongues are rather

small, so that significant instability exponents are found in the broad bases: for increasing Ω , the first encountered significant instability corresponds to a degree $n = 3$: for $\epsilon = 0$, the corresponding minimal value of Ω/ω is $(\frac{183+36\sqrt{30}}{599})^{1/2} = 0.79667\dots$ [30]. This is apparent in figure 3, where we plot the Lyapunov exponent as a function of Ω/ω for various degrees n and for $\epsilon = 0.1$.

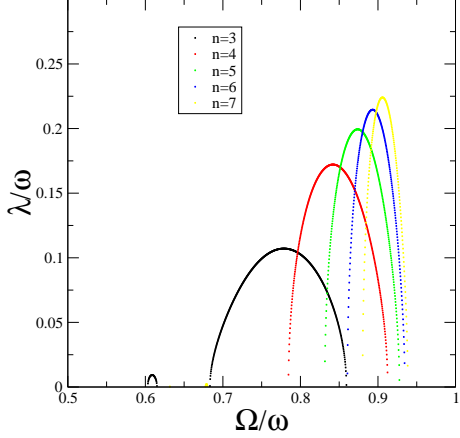


FIG. 3: For the upper branch of solution for the phase parameter: Lyapunov exponent of the dynamic instability for degrees n from 3 to 7, as a function of the rotation frequency. The trap anisotropy is $\epsilon = 0.1$.

III. NUMERICAL SOLUTION OF THE TIME DEPENDENT BCS EQUATIONS

We recall briefly the BCS equations for our two-component lattice model, in the case of equal populations of the two spin states. In the non-rotating case, the many-body ground of the Hamiltonian is approximated in BCS theory by the vacuum state of annihilation operators of elementary excitations, $b_{s,\sigma}$, constructed such that

$$\psi_{\uparrow}(\mathbf{r}) = \sum_s b_{s,\uparrow} u_s(\mathbf{r}) - b_{s,\downarrow}^{\dagger} v_s^*(\mathbf{r}) \quad (18)$$

$$\psi_{\downarrow}(\mathbf{r}) = \sum_s b_{s,\downarrow} u_s(\mathbf{r}) + b_{s,\uparrow}^{\dagger} v_s^*(\mathbf{r}) \quad (19)$$

where the u 's and v 's are all the eigenvectors of the following Hermitian system with positive energies $E_s > 0$:

$$E_s \begin{pmatrix} u_s \\ v_s \end{pmatrix} = \begin{pmatrix} h_0 & \Delta \\ \Delta^* & -h_0^* \end{pmatrix} \begin{pmatrix} u_s \\ v_s \end{pmatrix} \quad (20)$$

and normalized so that

$$l^2 \sum_{\mathbf{r}} |u_s(\mathbf{r})|^2 + |v_s(\mathbf{r})|^2 = 1. \quad (21)$$

In the eigensystem, Δ is the position dependent gap parameter defined in Eq.(10) and the matrix h_0 represents on the lattice the single particle kinetic energy plus

chemical potential plus harmonic potential energy terms. When the modal decomposition Eq.(19) is inserted in Eq.(10), one gets

$$\Delta(\mathbf{r}) = -g_0 \sum_s u_s(\mathbf{r}) v_s^*(\mathbf{r}). \quad (22)$$

The density profile of the spin up component is given by

$$\rho_{\uparrow}(\mathbf{r}) \equiv \langle \psi_{\uparrow}^{\dagger}(\mathbf{r}) \psi_{\uparrow}(\mathbf{r}) \rangle = \sum_s |v_s(\mathbf{r})|^2. \quad (23)$$

Note that, as usual in the BCS theory, we have omitted the Hartree-Fock mean field term [31].

To solve numerically the self-consistent stationary BCS equations, we have used the following iterative algorithm: one starts with an initial guess for the density profile and the gap parameter (we used the local density approximation, taking advantage of the fact that the equation of state and the value of the gap are known analytically in 2D [22]), then one calculates the u 's and v 's by diagonalization of the Hermitian matrix in Eq.(20), one calculates the corresponding ρ_{\uparrow} and Δ using Eq.(22) and Eq.(23), and one iterates until convergence.

Once the stationary BCS state is calculated, one moves to the solution of the time dependent BCS equations, to calculate the dynamics in the rotating trap. At time t , the modal expansion Eq.(19) still holds, with the operators $b_{s,\sigma}$ being constants of motion, except that the mode functions are now time dependent and evolve according to

$$i\hbar \partial_t \begin{pmatrix} u_s \\ v_s \end{pmatrix} = \begin{pmatrix} h_0 & \Delta \\ \Delta^* & -h_0^* \end{pmatrix} \begin{pmatrix} u_s \\ v_s \end{pmatrix} \quad (24)$$

where h_0 now includes the rotational term $-\Omega(t)L_z$ in addition to the kinetic energy, the chemical potential and the trapping potential. The gap function Δ is still given by Eq.(22) and is now time dependent as the mode functions are. We then integrated numerically Eq.(24); the usual FFT split technique, which exactly preserves the orthonormal nature of the u 's and v 's, is actually not sufficient because it assumes that the gap function remains constant in time during one time step, which breaks the self-consistency of the equations and leads to a violation of the conservation of the mean number of particles. We therefore used an improved splitting method detailed in the appendix B.

In all the simulations that we present here, the spatial grid was 32×32 , the trap anisotropy was $\epsilon = 0.1$. The chemical potential of the initial state of the gas was fixed to $\mu = 8\hbar\omega$; setting $\mu = \hbar^2 k_F^2 / 2m$, the 2D scattering length was fixed to the value $a_{2D} = (\hbar/m\omega)^{1/2} \equiv a_{ho}$ such that $k_F a_{2D} = 4$; the rotation frequency was turned on with the following law

$$\Omega(t) = \Omega \sin^2 \left(\frac{\pi t}{2\tau} \right) \quad \text{for } 0 \leq t \leq \tau \quad (25)$$

with a ramping time $\tau = 80\omega^{-1}$ much larger than the oscillation period of the atoms in the trap. For $t > \tau$, the

rotation frequency remains equal to Ω . The presence of vortices is detected by calculating the winding number of the phase of the gap parameter around each plaquette of the grid. We also calculated the total angular momentum of the spin \uparrow component of the gas.

We evolved the system for a total time of $1000 \omega^{-1}$. We varied the final rotation frequency in steps of 0.1ω . For final rotation frequencies $\Omega \leq 0.3\omega$, no vortices was found to enter the cloud and the cloud remains round. For $\Omega = 0.4\omega$, the cloud remains round but a corrugation of the surface of the cloud is observed and two diametrically opposite vortices enter the cloud gently and settle in a stationary pair of vortices close to the trap center. For $\Omega = 0.5\omega$, the situation is similar, except that 4 vortices at the corners of an approximate square enter, the radius of the square shrinking gradually until a stationary state is reached. Selected images of the movie of the simulation for $\Omega = 0.5\omega$ are shown in figure 4. Clearly, in these scenarios, no global turbulence of the cloud is involved, since the final regular vortex pattern is pre-formed when it enters the cloud. One observe that the entering vortex patterns obey the parity symmetry of the Hamiltonian.

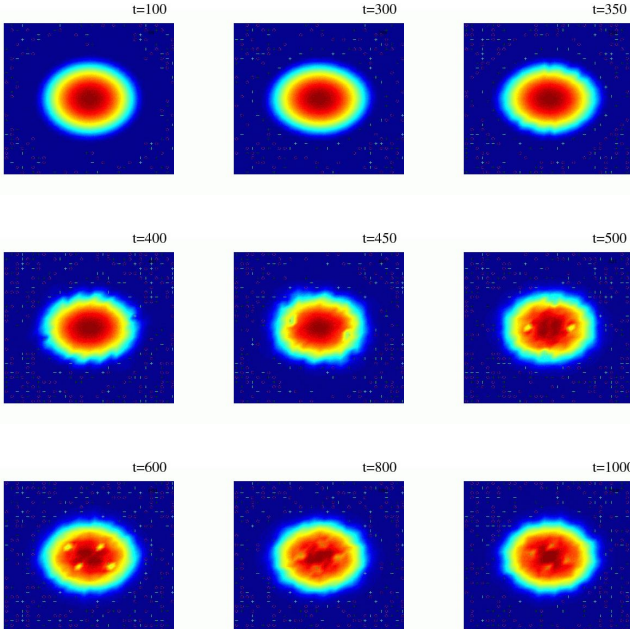


FIG. 4: For the numerical simulation of the time dependent BCS equations, density plots of the density of the trapped gas at selected times (in units of ω^{-1}), for a final rotation frequency $\Omega = 0.5\omega$. The trap anisotropy was $\epsilon = 0.1$ and the 2D scattering length $a_{2D} = \sqrt{\hbar/m\omega}$, and $\mu = 8\hbar\omega$ in the initial state. Crosses: positive charge vortices. Circles: negative charge vortices.

For $\Omega = 0.6\omega$, the scenario is slightly different. The corrugation of the surface is stronger, and a regular, parity invariant, pattern of 6 vortices enter, in two parallel rows. After some time, this pattern becomes hexagonal, then two more vortices enter, the 8 vortices settling in a

regular pattern. Then 2 extra vortices enter, and 2 again until a vortex lattice with 12 vortices is formed at the end of the simulation.

For $\Omega = 0.7\omega$ and $\Omega = 0.8\omega$ the dynamics is very different. The shape of the cloud strongly elongates and deforms, taking at some stage a S shape. Then strong turbulence sets in, breaking the parity invariance in the numerical simulation by an amplification of numerical noise, and leading to a quick entrance of several vortices and anti-vortices in the cloud. After some evolution time, the cloud recovers an elliptic shape, the anti-vortices are expelled from the cloud and the vortices settle in a stationary lattice. Selected images of the movie of the simulation for $\Omega = 0.8\omega$ are shown in figure 5. To briefly address the experimental observability of the vortex pattern, we also show in figure 6 a cut of the particle density (directly measurable in an experiment) and of the gap parameter (not directly accessible experimentally) for the simulation $\Omega = 0.8\omega$ at a time when the vortex lattice is quasi-formed, this in parallel to an isocontour of the magnitude of the gap parameter: one see that vortices embedded in high density regions result in dips in the density profile, which a contrast on the order here of 30%.

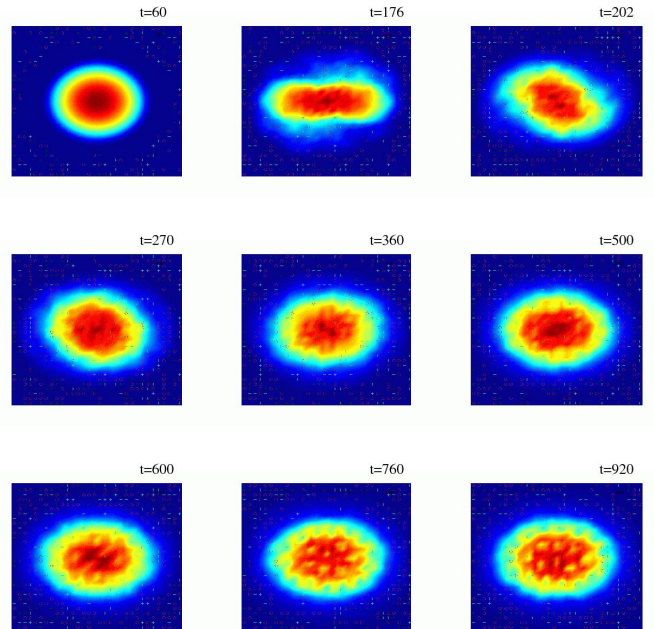


FIG. 5: For the numerical simulation of the time dependent BCS equations, density plots of the density of the trapped gas at selected times (in units of ω^{-1}), for a final rotation frequency $\Omega = 0.8\omega$. The trap anisotropy was $\epsilon = 0.1$ and the 2D scattering length $a_{2D} = \sqrt{\hbar/m\omega}$, and $\mu = 8\hbar\omega$ in the initial state. Crosses: positive charge vortices. Circles: negative charge vortices.

In conclusion, two distinct scenarios of vortex lattice formation are observed in the simulations. For the lower rotation frequencies, a gentle entry of an order pattern

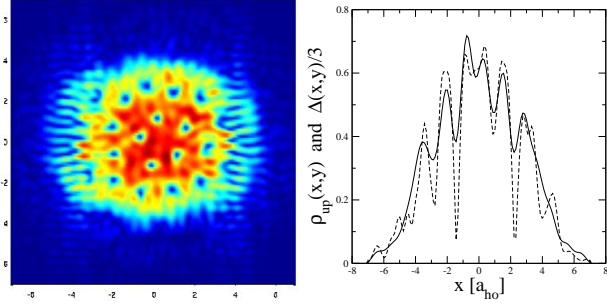


FIG. 6: At time $t = 548.3\omega^{-1}$ of the numerical simulation for $\Omega = 0.8\omega$. Left panel: isocontours of the modulus of the gap parameter, showing the presence of a vortex lattice. Right panel: on the line $y = 2.1a_{ho}$ (shown in blue on the left panel), x dependence of the density ρ_\uparrow (solid line, in units of a_{ho}^2) and of the gap parameter (dashed line, in units of $\hbar\omega$). The gap parameter was divided by 3 for clarity. A Fourier interpolation technique was used to map the 32×32 simulation grid onto a 128×128 grid.

of vortices is observed. For the higher rotation frequencies, turbulence sets in and leads to the abrupt and disordered entrance of vortices and even anti-vortices, the vortex lattice forming after a rather long evolution time. The physical origin of the turbulent scenario is expected to be the dynamic instability of the mode of degree $n = 3$ discussed in section II, and the obtained movies qualitatively agree with that. More quantitatively: for $\epsilon = 0.1$ a significant Lyapunov exponent is obtained for $\Omega > 0.68\omega$; this is compatible with the fact that the numerical simulation observes turbulence for $\Omega \geq 0.7\omega$ only.

What is the physical origin of the gentle scenario ? The observed corrugation at the surface suggests that it is driven by the instability of some surface mode localized at the surface of the cloud, which is reminiscent of the Landau mechanism. As a test of this idea, we have performed a numerical calculation of the stationary BCS state in a rotating frame, by the above mentioned iterative scheme: as shown in figure 7 giving the angular momentum of the stationary as function of the rotation frequency, for $\epsilon = 0.1$, the branch with no vortex is followed up to $\Omega = 0.3\omega$; for larger values of Ω , the algorithm jumps to a configuration with vortices. This suggests that the vortex free BCS state is indeed not a local minimum of energy for $\Omega > 0.3\omega$. What is then puzzling at this stage is that a harmonic stirrer can excite only the quadrupolar modes, whereas the negative energy surface mode initiating the Landau mechanism is expected to have a higher angular momentum [13]. A possible solution to this paradox was obtained by running the time dependent simulation with $\epsilon = 0$, for $\Omega = 0.5\omega$: in this case, the harmonic trap, being isotropic, can not stir the gas and the stirring is due only to the fixed periodic boundary conditions in the rotating frame; still, vortices were found to enter the cloud. This shows that the quantization box in our simulations is small enough

to activate the Landau mechanism; we therefore cannot be sure that it would take place in a purely harmonic trap. Elucidation of this point requires more detailed investigations beyond the scope of the present paper.

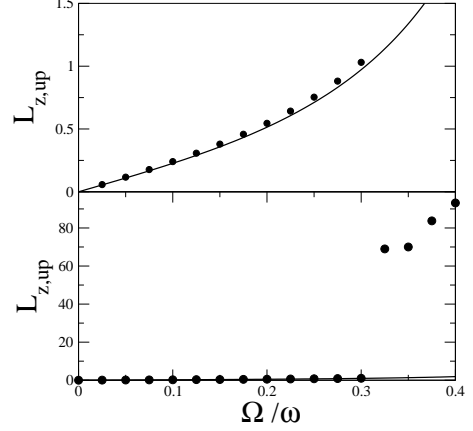


FIG. 7: In a steady state solution of the BCS theory, total angular momentum of the gas per spin component, in units of \hbar , as a function of the rotation frequency, for $\epsilon = 0.1$ and $\mu = 8h\omega$, $a = (\hbar/m\omega)^{1/2}$. Black disks: numerical result from an iterative algorithm (vortices present at the right part of the jump, no vortex at the left part of the jump). Solid line: hydrodynamic prediction (no vortex). The upper graph corresponds to the same data as the lower graph, but for a different scale of the vertical axis: it shows the good agreement of the hydrodynamic prediction with the full numerics. In the numerics, the number of spin \uparrow particles is ~ 36 on the left part of the jump, and reaches ~ 40 on the most right data point.

IV. CONCLUSION

We have investigated a relevant problem for the present experiments on two-spin component interacting Fermi gases, the possibility to form a vortex lattice by slow ramping of the rotation frequency of the harmonic trap containing the particles. The observation of a such a vortex lattice in steady state would be a very convincing evidence of superfluidity.

For a 2D model based on the BCS theory, we predict analytically, with the superfluid hydrodynamic equations, that the gas experiences a dynamic instability when the final rotation frequency is above some minimal value Ω_u that we have calculated. This dynamic instability is very similar to the one discovered for a rotating Bose-Einstein condensate of bosonic atoms, where it was shown to lead to the vortex lattice formation.

To see if this dynamic instability leads to the formation of vortices also in the case of the Fermi gases, we have solved numerically the full 2D time-dependent BCS equations, for a trap anisotropy $\epsilon = 0.1$. For a final rotation frequency Ω above the predicted Ω_u , we see turbulence and the subsequent fast entry of vortices. We conclude

that the dynamic instability can indeed result in a vortex lattice formation.

For $\Omega < \Omega_u$ but for Ω larger than what we estimated to be the Landau rotation frequency (above which the vortex free superfluid is no longer a local minimum of energy in the rotating frame), we also see the formation of a vortex lattice in the simulations, but with a gentle mechanism not involving turbulence and leading to the entrance of a pre-formed regular vortex pattern from the surface of the cloud. The elucidation of the corresponding mechanism requires more extensive simulations, since we have found that this mechanism is present at $\epsilon = 0$ (i.e. in the absence of trap anisotropy) in the present simulations, so that it may be enhanced or even induced by the rotating quantization box used in the numerics. In a real experiment, we expect such a mechanism to occur for a gas initially at finite temperature, when the normal component of the gas is set into rotation by the stirrer.

Acknowledgments

We acknowledge discussions with C. Salomon and A. Sinatra. Laboratoire Kastler Brossel is a Unité de Recherche de l'École Normale Supérieure et de l'Université Paris 6, associée au CNRS.

APPENDIX A: SIMPLE DERIVATION OF THE HYDRODYNAMIC EQUATIONS FROM BCS THEORY

We show here that the time dependent hydrodynamic equations Eq.(12) and Eq.(13) can be formally derived for a vortex free gas from the time dependent BCS equations by using the lowest order semi-classical approximation and an adiabatic approximation for the resulting time dependent equations. As in the remaining part of the paper, we consider here the regime where the chemical potential is positive and larger than the binding energy E_0 .

The general validity condition of a semi-classical approximation is that the coherence length of the gas should be much smaller than the typical length scales of variation of the applied potentials. Two coherence lengths appear for a zero temperature BCS Fermi gas: the inverse Fermi wave-vector, k_F^{-1} , and the pair size, $l_{\text{BCS}} \sim \hbar^2 k_F / m |\Delta|$. A first typical length scale of variation of the matrix elements in Eq.(24) comes from the position dependence of $|\Delta|$: in the absence of vortices, we assume that this is the Thomas-Fermi radius R_{TF} of the gas, defined as $\hbar^2 k_F^2 / 2m = m\omega^2 R_{\text{TF}}^2 / 2$. This assumes that the scale of variation of the modulus of the gap is the same as the one of the density; the adiabatic approximation to come will result in a $|\Delta|$ related to the density by Eq.(4), which justifies the assumption. Necessary validity conditions of a semi-classical approximation

are then:

$$k_F^{-1}, l_{\text{BCS}} \ll R_{\text{TF}}. \quad (\text{A1})$$

The presence of vortices introduces an extra length scale in the variation of $|\Delta|$, on the order of l_{BCS} , which invalidates the semi-classical approximation.

In the rotating case, however, this is not the whole story, as the phase of Δ can also become position dependent. As we shall see, the phase of Δ in this paper may vary as $m\omega xy/\hbar$: when this quantity varies by $\sim 2\pi$, Δ changes completely; this introduces a length scale $\sim 2\pi\hbar/(m\omega R_{\text{TF}}) \sim 1/k_F$, making a semi-classical approximation hopeless. We eliminate this problem by performing a gauge transform of the u 's and v 's:

$$\tilde{u}_s(\mathbf{r}, t) \equiv u_s(\mathbf{r}, t) e^{-iS(\mathbf{r}, t)/\hbar} \quad (\text{A2})$$

$$\tilde{v}_s(\mathbf{r}, t) \equiv v_s(\mathbf{r}, t) e^{+iS(\mathbf{r}, t)/\hbar} \quad (\text{A3})$$

where the phase is defined in Eq.(10). The time dependent BCS equations are modified as follows:

$$i\hbar\partial_t \begin{pmatrix} \tilde{u}_s \\ \tilde{v}_s \end{pmatrix} = \begin{pmatrix} \tilde{h}_0 & |\Delta| \\ |\Delta| & -\tilde{h}_0^* \end{pmatrix} \begin{pmatrix} \tilde{u}_s \\ \tilde{v}_s \end{pmatrix} \equiv \hat{L} \begin{pmatrix} \tilde{u}_s \\ \tilde{v}_s \end{pmatrix} \quad (\text{A4})$$

where the gauge transformed Hamiltonian is

$$\tilde{h}_0 = e^{-iS/\hbar} h_0 e^{+iS/\hbar} + \partial_t S. \quad (\text{A5})$$

Let us review relevant observables in the gauge transformed representation. First the gap equation is modified as

$$|\Delta| = -g_0 \sum_s \tilde{u}_s \tilde{v}_s^*. \quad (\text{A6})$$

Then the mean density in one spin component reads

$$\rho_{\uparrow} = \sum_s \tilde{v}_s \tilde{v}_s^*. \quad (\text{A7})$$

Last, we introduce the matter current $\mathbf{j}_{\uparrow}(\mathbf{r}, t)$ such that

$$\partial_t \rho_{\uparrow} + \text{div } \mathbf{j}_{\uparrow} = 0. \quad (\text{A8})$$

By using Eq.(A4) to calculate the time derivative of Eq.(A7), and by using the fact that Eq.(A6) imposes, by construction, that its right hand side sum is real, we obtain after lengthy but exact calculations:

$$\mathbf{j}_{\uparrow} = \rho_{\uparrow} (\mathbf{v} - \Omega \times \mathbf{r}) + \frac{i\hbar}{2m} \sum_s [\tilde{v}_s^* \mathbf{grad} \tilde{v}_s - \tilde{v}_s \mathbf{grad} \tilde{v}_s^*]. \quad (\text{A9})$$

To calculate the two key quantities Eq.(A7) and Eq.(A9), it is sufficient to know the following one-body density operator

$$\sigma = \sum_s \begin{pmatrix} |\tilde{u}_s\rangle\langle\tilde{u}_s| & |\tilde{u}_s\rangle\langle\tilde{v}_s| \\ |\tilde{v}_s\rangle\langle\tilde{u}_s| & |\tilde{v}_s\rangle\langle\tilde{v}_s| \end{pmatrix}. \quad (\text{A10})$$

To prepare for the semi-classical approximation we introduce the Wigner representation of σ :

$$W(\mathbf{r}, \mathbf{p}, t) = \text{Wigner}\{\sigma\} \equiv \int \frac{d^d \mathbf{x}}{(2\pi\hbar)^d} \langle \mathbf{r} - \mathbf{x}/2 | \sigma | \mathbf{r} + \mathbf{x}/2 \rangle e^{i\mathbf{p} \cdot \mathbf{x}/\hbar} \quad (\text{A11})$$

where d is the dimension of space. The key observables have then the exact expressions:

$$\rho_{\uparrow}(\mathbf{r}, t) = \int \frac{d^d \mathbf{p}}{\hbar^d} W_{\uparrow\uparrow}(\mathbf{r}, \mathbf{p}, t) \quad (\text{A12})$$

$$|\Delta|(\mathbf{r}, t) = -g_0 \int \frac{d^d \mathbf{p}}{\hbar^d} W_{\uparrow\downarrow}(\mathbf{r}, \mathbf{p}, t) \quad (\text{A13})$$

$$\mathbf{j}_{\uparrow}(\mathbf{r}, t) = \rho_{\uparrow}(\mathbf{v} - \Omega \times \mathbf{r}) - \frac{1}{m} \int \frac{d^d \mathbf{p}}{\hbar^d} \mathbf{p} W_{\uparrow\uparrow}(\mathbf{r}, \mathbf{p}, t) \quad (\text{A14})$$

The semi-classical expansion then consists e.g. in

$$\text{Wigner}\{V(\hat{\mathbf{r}})\sigma\} = [V(\mathbf{r}) + \frac{i\hbar}{2} \partial_{\mathbf{r}} V \cdot \partial_{\mathbf{p}} + \dots] W(\mathbf{r}, \mathbf{p}, t). \quad (\text{A15})$$

The successive terms we called zeroth order, first order, etc, in the semi-classical approximation.

We write the equations of motion Eq.(A4) up to zeroth order in the semi-classical approximation:

$$i\hbar \partial_t W(\mathbf{r}, \mathbf{p}, t)|^{(0)} = [L(\mathbf{r}, \mathbf{p}, t), W(\mathbf{r}, \mathbf{p}, t)] \quad (\text{A16})$$

where the matrix L corresponds to the classical limit of the operator \hat{L} and is equal to

$$L = \begin{pmatrix} \frac{p^2}{2m} - \mu_{\text{eff}} & |\Delta| \\ |\Delta| & -\frac{p^2}{2m} + \mu_{\text{eff}} \end{pmatrix} + \mathbf{v} \cdot \mathbf{p} - \Omega \cdot (\mathbf{r} \times \mathbf{p}) \quad (\text{A17})$$

where the position and time dependent effective chemical potential is

$$\mu_{\text{eff}}(\mathbf{r}, t) \equiv \mu - U(\mathbf{r}, t) - \frac{1}{2}mv^2 + \mathbf{m} \cdot (\Omega \times \mathbf{r}) - \partial_t S(\mathbf{r}, t) \quad (\text{A18})$$

where the name effective chemical potential will become clear soon.

At time $t = 0$, the gas is at zero temperature. By introducing the spectral decomposition of $\hat{L}(t = 0)$ one can then check that

$$\sigma(t = 0) = \theta[\hat{L}(t = 0)] \quad (\text{A19})$$

where $\theta(x)$ is the Heaviside function. The leading order semi-classical approximation for the corresponding Wigner function is, in a standard way, given by

$$W(\mathbf{r}, \mathbf{p}, t = 0) \simeq \theta[L(\mathbf{r}, \mathbf{p}, t = 0)] \quad (\text{A20})$$

that is each two by two matrix W is a pure state $|\psi\rangle\langle\psi|$ with

$$|\psi(\mathbf{r}, \mathbf{p}, t = 0)\rangle = \begin{pmatrix} U_0(\mathbf{r}, \mathbf{p}) \\ V_0(\mathbf{r}, \mathbf{p}) \end{pmatrix} \quad (\text{A21})$$

where (U_0, V_0) is the eigenvector of $L(\mathbf{r}, \mathbf{p}, t = 0)$ of positive energy and normalized to unity. At time t , according to the zeroth order evolution Eq.(A16), each two by two matrix W remains a pure state, with components U and V solving

$$i\hbar \partial_t \begin{pmatrix} U(\mathbf{r}, \mathbf{p}, t) \\ V(\mathbf{r}, \mathbf{p}, t) \end{pmatrix} = L(\mathbf{r}, \mathbf{p}, t) \begin{pmatrix} U(\mathbf{r}, \mathbf{p}, t) \\ V(\mathbf{r}, \mathbf{p}, t) \end{pmatrix} \quad (\text{A22})$$

We then introduce the so-called adiabatic approximation: the vector (U, V) , being initially an eigenstate of $L(\mathbf{r}, \mathbf{p}, t = 0)$, will be an instantaneous eigenvector of $L(\mathbf{r}, \mathbf{p}, t)$ at all later times t , provided that the matrix elements of $L(\mathbf{r}, \mathbf{p}, t)$ vary with temporal frequencies much smaller than the energy difference between the two eigenvalues of $L(\mathbf{r}, \mathbf{p}, t)$ (divided by \hbar). As this energy difference is larger than the gap parameter, this will impose a minimal value to the gap, as we shall discuss later. In this adiabatic approximation, one can take

$$W(\mathbf{r}, \mathbf{p}, t) = |+\rangle\langle+| \quad (\text{A23})$$

where $|+\rangle$, of real components $(U_{\text{inst}}, V_{\text{inst}})$, is the instantaneous eigenvector of the matrix

$$\begin{pmatrix} \frac{p^2}{2m} - \mu_{\text{eff}}(\mathbf{r}, t) & |\Delta|(\mathbf{r}, t) \\ |\Delta|(\mathbf{r}, t) & -\frac{p^2}{2m} + \mu_{\text{eff}}(\mathbf{r}, t) \end{pmatrix} \quad (\text{A24})$$

with positive eigenvalue. Note that it is also an eigenvector of $L(\mathbf{r}, \mathbf{p}, t)$, and that its components are simply the amplitudes on the plane wave $\exp(ip \cdot r/\hbar)$ of the BCS mode functions of a spatially uniform BCS gas of chemical potential μ_{eff} and of gap parameter $|\Delta(\mathbf{r}, t)|$. Using Eq.(A12) and Eq.(A13) with the approximate Wigner distribution Eq.(A23), one further finds that this fictitious spatially uniform BCS gas is at equilibrium at zero temperature so that the expressions Eq.(2) and Eq.(4) may be used. In particular, Eq.(2) gives

$$\mu_{\text{eff}}(\mathbf{r}, t) = \mu_0[\rho_{\uparrow}(\mathbf{r}, t)] \quad (\text{A25})$$

which leads, together with Eq.(A18), to one of the time dependent hydrodynamic equations, the Euler-type one Eq.(13). Also, U_{inst} and V_{inst} are even functions of \mathbf{p} , so that the integral in the right hand side of Eq.(A14) vanishes and Eq.(A8) reduces to the hydrodynamic continuity equation Eq.(12).

We now discuss the validity of the adiabatic approximation. Without this approximation, the two by two matrix W has non-zero off-diagonal matrix elements $\langle +|W|-\rangle$ where $|-\rangle$ is the instantaneous eigenvector of Eq.(A24) with a negative eigenvalue, that can be written $(V_{\text{inst}}, -U_{\text{inst}})$. Writing from Eq.(A16) the equation of motion for $\langle +|W|-\rangle$, one finds a coupling to the diagonal element $\langle +|W|+\rangle$ due to the non infinite ramping time of the rotation and corresponding to a Rabi frequency that can be calculated using the off-diagonal Hellman-Feynman theorem for real eigenvectors:

$$\frac{1}{2} \nu_{\text{ramp}} \equiv \langle -|\partial_t|+ \rangle = \frac{1}{\epsilon_+ - \epsilon_-} \langle -|(\partial_t L)|+ \rangle \quad (\text{A26})$$

where ϵ_{\pm} is the eigenenergy of $|\pm\rangle$ for the full matrix L :

$$\epsilon_{\pm} = \mathbf{p} \cdot (\mathbf{v} - \Omega \times \mathbf{r}) \pm \left[\left(p^2/(2m) - \mu_{\text{eff}} \right)^2 + |\Delta|^2 \right]^{1/2}. \quad (\text{A27})$$

We calculate ν_{ramp} when $p^2/2m = \mu_{\text{eff}}$, where the energy difference is minimal and equal to twice the gap; then $U_{\text{inst}} = V_{\text{inst}} = 1/\sqrt{2}$ and the Rabi frequency due to a finite ramping time of the rotation is

$$\nu_{\text{ramp}} = -\frac{\partial_t \mu_{\text{eff}}}{|\Delta|}. \quad (\text{A28})$$

Adiabaticity requires the value of $\nu_{\text{ramp}}/2$ to be much smaller than $2|\Delta|/\hbar$. Setting in 2D $\partial_t \mu_{\text{eff}} \sim \tau^{-1} \times 2\pi\hbar^2 \rho_{\uparrow}/m$, where τ is the ramping time of the rotation frequency, and using Eq.(4) we arrive at the simple condition on the ramping time:

$$8E_0\tau/\hbar \gg 1. \quad (\text{A29})$$

which is well satisfied in our simulations but which differs from the expected condition $|\Delta|\tau \gg \hbar$.

This discussion of validity is actually incomplete, as it neglects so-called motional couplings, due to the fact that $|+\rangle$ and $|-\rangle$ depends on \mathbf{r}, \mathbf{p} and that terms involving $\partial_{\mathbf{p}}W$ and $\partial_{\mathbf{r}}W$ will appear in the equation for W beyond the zeroth-order semi-classical approximation. Such motional effects are well known for the motion of a spin 1/2 particle in a static but spatially inhomogeneous magnetic field and can lead to the fact that the spin state no longer follows adiabatically the direction of the magnetic field. In our problem, the first order term of the semi-classical expansion is actually simple to write:

$$i\hbar\partial_t W|^{(1)} = \frac{1}{2} [\partial_{\mathbf{r}}L \cdot \partial_{\mathbf{p}}W - \partial_{\mathbf{p}}L \cdot \partial_{\mathbf{r}}W + \text{h.c.}]. \quad (\text{A30})$$

In the resulting equation of evolution of $\langle +|W|-\rangle$, a motional Rabi coupling to $\langle +|W|+\rangle$ now appears:

$$\frac{1}{2}\nu_{\text{motion}} \equiv \frac{1}{2} [\partial_{\mathbf{p}}(\epsilon_{+} + \epsilon_{-}) \cdot \langle -|\partial_{\mathbf{r}}|+ \rangle - \partial_{\mathbf{r}}(\epsilon_{+} + \epsilon_{-}) \cdot \langle -|\partial_{\mathbf{p}}|+ \rangle]. \quad (\text{A31})$$

Evaluating this Rabi frequency when $p^2/2m = \mu_{\text{eff}}$, and using the hydrodynamic equations of motion plus the specific fact that the velocity field is the gradient of $\omega_{\perp}\beta_{xy}$ (see Eq.(14), valid in steady state that is here for a ramping time τ that tends to infinity), we get, thanks to the Hellman-Feynman theorem, the remarkably simple expression for the Rabi frequency purely due to motional coupling:

$$\frac{1}{2}\nu_{\text{motion}} = -\frac{\beta\omega p_x p_y}{m|\Delta|}. \quad (\text{A32})$$

The constraint $\nu_{\text{motion}}/2 \ll 2|\Delta|/\hbar$ then results in the condition for negligible motional non-adiabatic effects, in 2D:

$$\hbar\omega \ll 2E_0/\beta. \quad (\text{A33})$$

This condition is satisfied in our simulations as β is at most ~ 0.64 (for $\Omega = 0.8\omega$) and we took $a = (\hbar/m\omega)^{1/2}$, $\mu = 8\hbar\omega$ resulting in $E_0 \sim 1.3\hbar\omega$ and $\Delta \sim 4.7\hbar\omega$. Note that it is in general more stringent than the condition $\hbar\omega \ll |\Delta|$ ensuing from $l_{\text{BCS}} \ll R_{\text{TF}}$ but for the particular parameters of our simulations, it turns out to be roughly equivalent.

APPENDIX B: A SPLITTING TECHNIQUE CONSERVING THE MEAN NUMBER OF PARTICLES

The standard splitting technique approximates the evolution due to Eq.(24) during a small time step dt by first evolving with the kinetic energy and rotational energy during dt , and then evolving with the \mathbf{r} -dependent part of two by two matrix of Eq.(24) during dt for a fixed value of $\Delta(\mathbf{r}, t)$. This exactly preserves the unitary of the full evolution, but it breaks the self-consistency between Δ and u_s, v_s so that the total number of spin \uparrow particles, $N_{\uparrow} = \sum_s \langle v_s | v_s \rangle$, is not exactly conserved. Numerically, one then observes strong deviations of this total number from its initial value.

This problem can be fixed by restoring the self-consistency for the evolution during dt due to the \mathbf{r} -dependent part of the equation of evolution. That is one solves during dt :

$$i\hbar\partial_t \begin{pmatrix} u_s \\ v_s \end{pmatrix} = \begin{pmatrix} U(\mathbf{r}) - \mu & \Delta \\ \Delta^* & \mu - U(\mathbf{r}) \end{pmatrix} \begin{pmatrix} u_s \\ v_s \end{pmatrix} \quad (\text{B1})$$

while keeping the self-consistency condition Eq.(22). Since this is purely local in \mathbf{r} , this can be done analytically. One finds that $\Delta(\mathbf{r}, t)$ varies as $e^{-i\lambda(\mathbf{r})t}$, where

$$\hbar\lambda(\mathbf{r}) = 2[U(\mathbf{r}) - \mu] - g_0 \sum_s |v_s(\mathbf{r}, t)|^2 - |u_s(\mathbf{r}, t)|^2 \quad (\text{B2})$$

can be checked to be time independent for the local evolution Eq.(B1). Then the system Eq.(B1) is transformed into one with time independent coefficients (so readily integrable) by switching to the rotating frame, $u_s(\mathbf{r}, t) = U_s(\mathbf{r}, t)e^{-i\lambda(\mathbf{r})t/2}$ and $v_s(\mathbf{r}, t) = V_s(\mathbf{r}, t)e^{+i\lambda(\mathbf{r})t/2}$.

[1] K.M. O'Hara, S.L. Hemmer, M.E. Gehm, S.R. Granade, J.E. Thomas, *Science* **298**, 2179 (2002).

[2] T. Bourdel, J. Cubizolles, L. Khaykovich, K. M. F. Magalhães, S. J. J. M. F. Kokkelmans, G. V. Shlyapnikov, C. Salomon, *Phys. Rev. Lett.* **91**, 020402 (2003).

[3] A. G. Leggett, *J. Phys. (Paris) C* **7**, 19 (1980); P. Nozières, S. Schmitt-Rink, *J. Low Temp. Phys.* **59**, 195 (1985); J. R. Engelbrecht, M. Randeria, and C. Sá de Melo, *Phys. Rev. B* **55**, 15153 (1997).

[4] M. Greiner, C. A. Regal, D. S. Jin, *Nature* **426**, 537 (2003); S. Jochim, M. Bartenstein, A. Altmeyer, G. Hendl, S. Riedl, C. Chin, J. Hecker Denschlag, R. Grimm, *Science* **302**, 2101 (2003); M. W. Zwierlein, C. A. Stan, C. H. Schunck, S. M. F. Raupach, S. Gupta, Z. Hadzibabic, W. Ketterle, *Phys. Rev. Lett.* **91**, 250401 (2003); T. Bourdel, L. Khaykovich, J. Cubizolles, J. Zhang, F. Chevy, M. Teichmann, L. Tarruell, S.J.J.M.F. Kokkelmans, C. Salomon, *Phys. Rev. Lett.* **93**, 050401 (2004).

[5] C. A. Regal, M. Greiner, and D. S. Jin, *Phys. Rev. Lett.* **92**, 040403 (2004); M. W. Zwierlein, C. A. Stan, C. H. Schunck, S. M. F. Raupach, A. J. Kerman, W. Ketterle, *Phys. Rev. Lett.* **92**, 120403 (2004).

[6] C. Chin, M. Bartenstein, A. Altmeyer, S. Riedl, S. Jochim, J. Hecker Denschlag, R. Grimm, *Science* **305**, 1128 (2004).

[7] P. Törmä, P. Zoller, *Phys. Rev. Lett.* **85**, 487 (2000).

[8] C. Menotti, P. Pedri, S. Stringari, *Phys. Rev. Lett.* **89**, 250402 (2002).

[9] M. Cozzini, S. Stringari, *Phys. Rev. Lett.* **91**, 070401 (2003).

[10] D. L. Feder, *Phys. Rev. Lett.* **93**, 200406 (2004).

[11] N. Nygaard, G. M. Bruun, C. W. Clark, D. L. Feder, *Phys. Rev. Lett.* **90**, 210402 (2003).

[12] T. Isoshima, K. Machida, *Phys. Rev. A* **60**, 3313 (1999).

[13] F. Dalfovo and S. Stringari, *Phys. Rev. A* **63**, 011601(R) (2000).

[14] K. W. Madison, F. Chevy, W. Wohlleben, and J. Dalibard, *Phys. Rev. Lett.* **84**, 806 (2000).

[15] S. Sinha, Y. Castin, *Phys. Rev. Lett.* **87**, 190402 (2001).

[16] K. Madison, F. Chevy, V. Bretin, and J. Dalibard, *Phys. Rev. Lett.* **86**, 4443 (2001).

[17] E. Hodby, G. Hechenblaikner, S.A. Hopkins, O.M. Maragò, C.J. Foot, *Phys. Rev. Lett.* **88**, 010405 (2002).

[18] D. L. Feder, A. A. Svidzinsky, A. L. Fetter, C. W. Clark, *Phys. Rev. Lett.* **86**, 564 (2001).

[19] C. Lobo, A. Sinatra, Y. Castin, *Phys. Rev. Lett.* **92**, 020403 (2004).

[20] D. S. Petrov and G. V. Shlyapnikov, *Phys. Rev. A* **64**, 012706 (2001); G. Shlyapnikov, *J. Phys. IV France* **116**, p.89-132 (2004).

[21] L. Pricoupenko, M. Olshanii, *cond-mat/0205210*.

[22] M. Randeria, J. Duan, and L. Shieh, *Phys. Rev. B* **41**, 327-343 (1990).

[23] C. Mora, Y. Castin, *Phys. Rev. A* **67**, 053615 (2003).

[24] Y. Castin, *J. Phys. IV France* **116**, p.89-132 (2004).

[25] G. Tonini, "Study of Ultracold Fermi gases: crystalline LOFF phase and nucleation of vortices", PhD thesis of the University of Florence (Italy).

[26] This last statement is actually not exactly true. Since the number of particles is conserved during the time evolution, the instantaneous chemical potential does not coincide with the initial one μ . One should set $\partial_t S = \delta\mu S$ where $\mu + \delta\mu$ is the true instantaneous chemical potential. For simplicity we ignore this subtlety here, with no consequence.

[27] A. Recati, F. Zambelli and S. Stringari, *Phys. Rev. Lett.* **86**, 377 (2001).

[28] In this figure, it is not apparent that the very narrow tongues actually touch the $\epsilon = 0$ axis; but this can be shown analytically, and the contact points are $\Omega = \omega/\sqrt{n}$, which is the value of the rotation frequency ensuring the resonance of the rotating anisotropy with the surface mode of frequency $\sqrt{n}\omega$ in the lab frame [29]. Note also that the degrees $n = 6$ and $n = 7$ (not shown in the figure) have each an additional instability zone, however with very low values of the Lyapunov exponent ($\sim 0.01\omega$) so of little physical relevance. We have not explored $n \geq 8$.

[29] S. Sinha, private communication.

[30] This value is obtained from the following result: the boundaries of the crescent of degree $n = 3$ can be parametrized as $\epsilon = \pm z_0(-z_0^2 + 2\Omega^2 - 1)/\Omega$ where z_0 is a root of the degree 5 polynomial $P(z) = 3z^5 + 19\Omega z^4 + (6 - 13\Omega^2)z^3 + (26\Omega - 25\Omega^3)z^2 + (3 + 3\Omega^4 - 10\Omega^2)z + 3\Omega^5 - 22\Omega^3 + 7\Omega$, Ω being expressed in units of ω .

[31] The mean field term is simply $g_0\rho_\uparrow$. It tends to zero in the limit of a grid spacing l tending to zero, both in the 3D and 2D BCS theories. In 2D however, this convergence is only logarithmic so can never be achieved in a practical numerical calculation. Keeping this mean field term introduces a spurious dependence on l in the BCS equation of state. This, as we have checked numerically, leads to a spurious dependence on l of the density profile and the gap parameter for a stationary gas in the trap in the BCS approximation: we have therefore removed the mean field term. In an exact many-body theory, not relying on the Born approximation as the Hartree-Fock mean field term does, we do not expect such a pathology to take place.